

The Third Ambient Aspirin Polymorph

Alexander G. Shtukenberg,[†] Chunhua T. Hu,[†] Qiang Zhu,^{*,‡} Martin U. Schmidt,[§] Wenqian Xu,^{||} Melissa Tan,[†] and Bart Kahr^{*,†,⊥}

[†]Department of Chemistry and Molecular Design Institute, New York University, 100 Washington Square East, Room 1001, New York City, New York 10003, United States

[‡]Department of Physics and Astronomy, High Pressure Science and Engineering Center, University of Nevada, Las Vegas, Las Vegas, Nevada 89154, United States

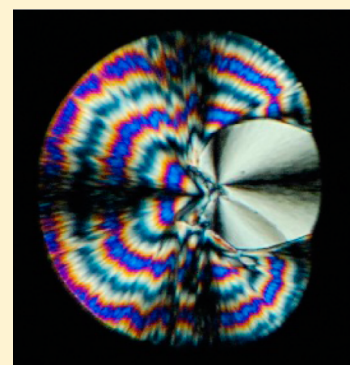
[§]Institute of Inorganic and Analytical Chemistry, Goethe University, Max-von-Laue-Strasse 7, 60438 Frankfurt am Main, Germany

^{||}X-ray Science Division, Advanced Photon Source, Argonne National Laboratory, Argonne, Illinois 60439, United States

[⊥]Department of Advanced Science and Engineering (TWins), Waseda University, Tokyo 162-0056, Japan

Supporting Information

ABSTRACT: Polymorphism of aspirin (acetylsalicylic acid), one of the most widely consumed medications, was equivocal until the structure of a second polymorph II, similar in structure to the original form I, was reported in 2005. Here, the third ambient polymorph of aspirin is described. It was crystallized from the melt, and its structure was determined using a combination of X-ray powder diffraction analysis and crystal structure prediction algorithms.



The synthesis of aspirin by acetylation of salicylic acid and its subsequent crystallization has been part of the training of many a chemist for generations.¹ Although a second polymorph was considered almost 50 years ago,² no structural information was available until 2005 when Zaworotko, Peterson, and co-workers solved the aspirin II crystal structure.³ This form had been anticipated by crystal structure prediction (CSP), but given the fact that phases I and II are merely polytypes distinguished by a small lateral shift of layers, the independent existence of phase II was not assured.⁴ It was later shown that phases I and II are frequently intergrown.^{5–7} Pure phase II was ultimately prepared.⁸ Aspirin III was observed by compressing phase I above 2 GPa, evidenced by the sudden changes in Raman spectra,⁹ but its crystal structure was not determined. Upon release of pressure, aspirin III transformed back to phase I, indicating that the high pressure phase is not recoverable at ambient conditions. Here, we report the preparation and structure of a third polymorph at ambient conditions, necessarily designated aspirin phase IV, a serendipitous consequence of our studies on crystals that twist as they grow.^{10–13}

Crystals growing under high driving force, for example at large undercoolings, develop large aspect ratios and commonly exhibit instabilities that direct the helicoidal twisting of propagating lamellae. This twisting typically manifests as concentric optical rings between crossed polarizers in so-called

banded spherulites.¹⁴ A few milligrams of aspirin (Sigma-Aldrich lot 081M0194V or Spectrum lot 2AI0521) was melted ($T_m = 133\text{ }^\circ\text{C}$) between glass slides on a hot plate to form a ca. $5\text{ }\mu\text{m}$ film. This melt undergoes spontaneous crystallization at room temperature to give aspirin I as striking banded spherulites^{12,13} (Figure 1). These structures are accompanied by a small fraction (<15%) of radially smooth, optically negative spherulites with lower birefringence, $N_z - N_x = 0.06(1)$ (Figure 1). The spherulites of the unknown phase (smooth spherulites) were metastable and converted to aspirin I within a couple of minutes at room temperature. The transformation can be slowed to ca. 1 h if, prior to melting, aspirin is mixed with 10–20% of Canada balsam, polyvinylpyrrolidone, or mannitol (Figure S1). At $4\text{ }^\circ\text{C}$, aspirin IV can be stored for ca. 1 day. The Raman spectrum of aspirin IV is distinct (Figure 2). An X-ray powder diffraction pattern was collected at room temperature with a Bruker AXS D8 DISCOVER GADDS microdiffractometer (Cu $K\alpha$ radiation, $\lambda = 1.54178\text{ }\text{Å}$) equipped with a VÅNTEC-2000 two-dimensional detector and a 0.5 mm MONOCAP collimator, the sample–detector distance was 150 mm in reflection mode. It revealed one maximum corresponding to $d = 7.9\text{ }\text{Å}$ absent in the powder patterns of aspirins I and II that disappears with the

Received: May 12, 2017

Published: May 17, 2017

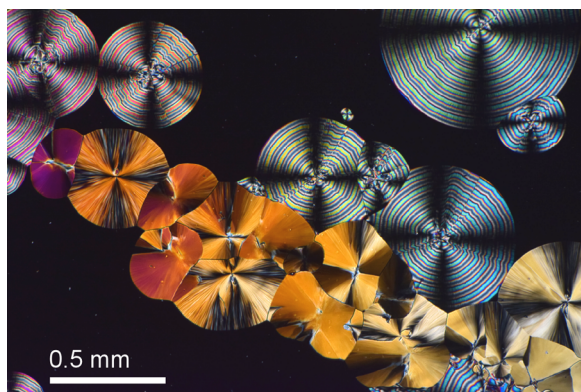


Figure 1. Polarized light micrograph showing simultaneous crystallization of banded spherulites of aspirin I and/or II characterized by concentric rings and smooth spherulites of aspirin IV from the melt containing 16.6 wt % Canada balsam at room temperature.

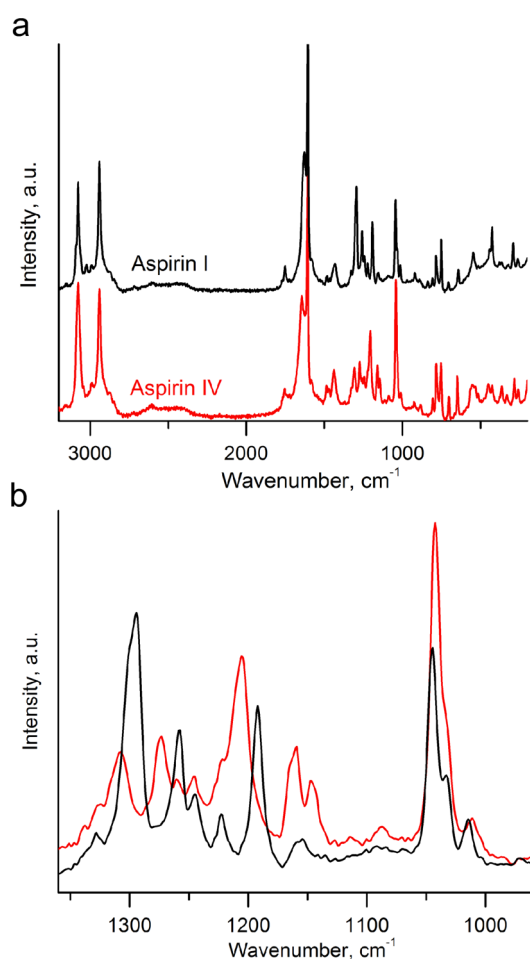


Figure 2. (a) Raman spectra of aspirin I (black line) and aspirin IV (red line) collected from aspirin spherulites grown from the melt at room temperature with 16.6 wt % Canada balsam. (b) Enlarged part of panel a showing the strongest differences between the two polymorphs. Canada balsam, present in samples of both polymorphs, does not form sharp Raman peaks (Figure S2) and thereby does not interfere with spectra of crystalline aspirin.

concomitant growth of aspirin I reflections. In the aggregate, these findings indicated the formation of an unknown phase (aspirin IV).

A more complete diffraction pattern of aspirin IV was obtained for samples crystallized in situ in a 0.8 mm diameter Kapton capillary mounted on a goniometer head of a Bruker SMART APEXII single crystal diffractometer (Mo $K\alpha$ radiation, $\lambda = 0.71073$ Å) equipped with a two-dimensional detector and an Oxford Systems 700+ Cooler; the sample–detector distance was 150 mm. Aspirin powder was melted inside a capillary and was rapidly quenched to the crystallization temperature of 240–255 K. To promote crystallization, samples were heated to 255–260 K for several minutes. X-ray diffraction patterns were collected every 5–30 min to follow the crystallization progress (Figure 3). Depending on the holding temperature, crystallization of half of the sample volume took 0.1–20 h (Figure S3). The fraction of aspirin IV mixed with aspirin I varied from 10 to 60%. This fraction reached its maximum after crystallization of approximately one-third of the sample volume because of aspirin IV \rightarrow I conversion at later stages.

Because the angular resolution of our local X-ray data was not sufficient for indexing and structure solution, we collected high-resolution diffraction data at the 17-BM beamline ($\lambda = 0.45336$ Å) of the Advanced Photon Source, Argonne National Laboratory. The experiment that produced the largest fraction of aspirin IV was selected for further analysis (see the Supporting Information for details). Neither of these 2D diffraction images showed preferential orientations of crystallites (Figure S4). The diffraction pattern was indexed using the software McMaille.¹⁵ We obtained a monoclinic cell with $a = 16.737(7)$ Å, $b = 4.797(2)$ Å, $c = 23.642(11)$ Å, $\beta = 110.21(2)^\circ$, and $V = 1781.2$ Å³ that corresponded to $Z = 8$. A similar result was obtained using the programs DICVOL¹⁶ and TOPAS.¹⁷

With these lattice parameters, the structure was solved using crystal structure search based on evolutionary CSP algorithms, as implemented in USPEX.^{18,19} As for the case of monoclinic glycine dihydrate,²⁰ we performed two independent crystal structure searches based on the experimentally determined cell, one with $Z' = 2$ in the space groups of $P2_1/c$, Cc , and $C2$ and the other with $Z' = 4$ in $P2_1$ and Pc . In our evolutionary search, the first generation of structures was created randomly in the given space groups. All structures were relaxed at ambient pressure and 0 K, and the enthalpy was used as fitness. The structures with the worst fitness (40%) were discarded, and a new generation was created as daughters from the rest of the structures in the pool based on different structure variation protocols. We generally terminated the runs after 50 generations. During the geometry optimization, all structures were first optimized by the CHARMM code²¹ with the force field generated from the CGENFF program^{22,23} via the online server (<http://cgenff.paramchem.org>), then followed by further relaxation at the level of density functional tight binding with the DFBT+ code²⁴ and 3ob-3-1 parameter set.²⁵ The 50 lowest-energy structures from the initial search were selected, and their geometries and energies were reoptimized with the VASP code.²⁶ To account for the missing van der Waals (vdW) interactions in the DFT framework, a vdW-inclusive model of optB88 was used.²⁷ A plane wave kinetic energy cutoff of 1000 eV was used, and the Brillouin zone was sampled by uniform Γ -centered meshes with the reciprocal space resolution at least $2\pi \times 0.06$ Å with convergence criteria of 1×10^{-5} eV/atom for total energies and 5×10^{-3} eV/Å for forces. Among the final 50 low-energy structures, the calculated powder pattern of the lowest-energy structure was in excellent agreement with the

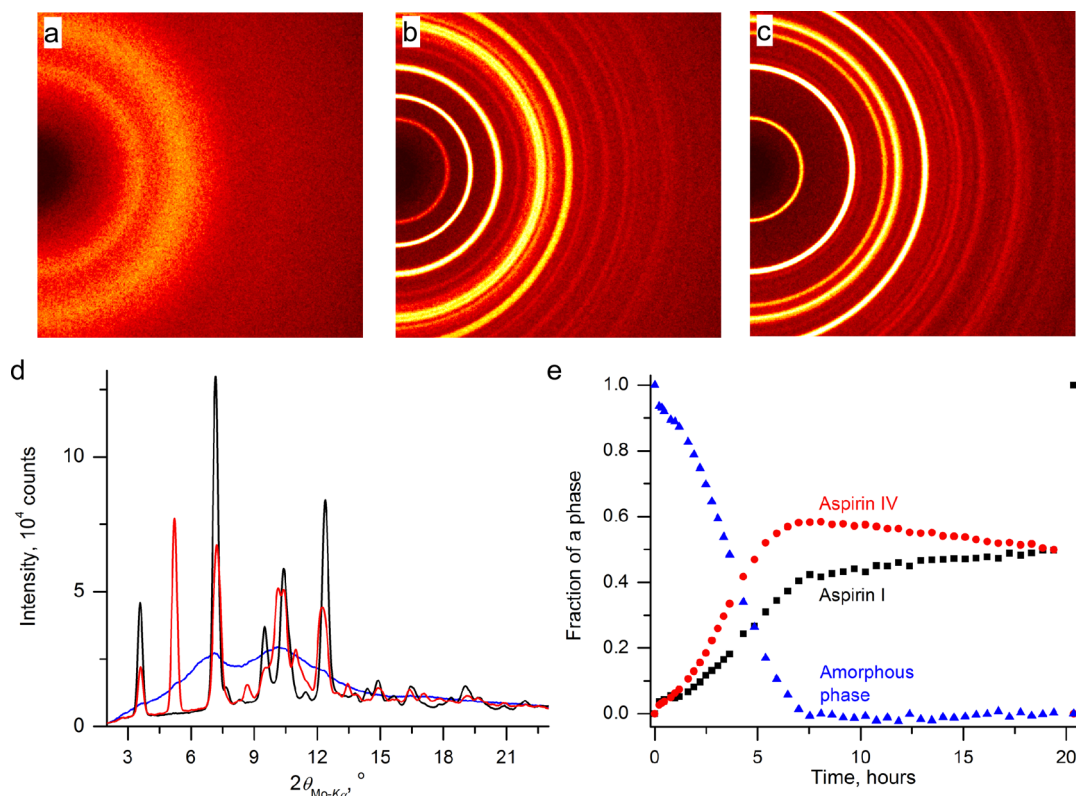


Figure 3. X-ray powder diffraction patterns collected at 250 K with an APEXII diffractometer at the beginning of crystallization (time = 0.12 h; panel a and blue line in panel d), after crystallization of the amorphous phase (time = 8.5 h; panel b and red line in panel d), and after conversion of the entire sample to aspirin I at 280 K (time = 20.4 h; panel c and black line in panel d). (e) Approximate mole fractions of aspirin I, aspirin IV, and the amorphous phase as a function of time estimated from the intensities of diffraction maxima for the experiment illustrated in panel d.

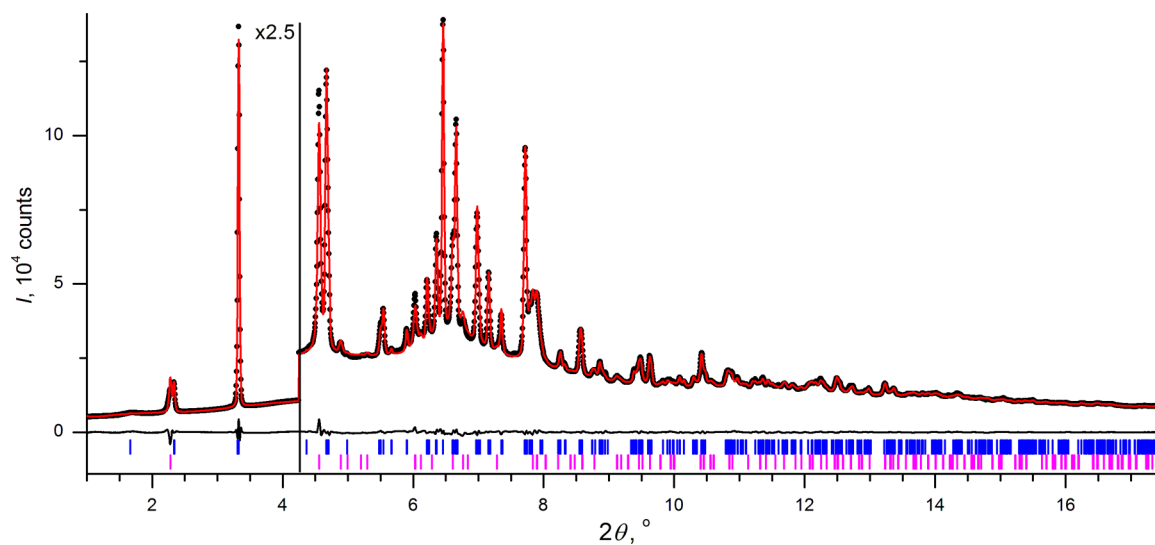


Figure 4. Rietveld refinement of high-resolution synchrotron powder diffraction data for an aspirin sample collected at the APS at a wavelength of 0.45336 Å and 255 K. Observed intensities, black circles; calculated intensities, red lines. Difference curve below. Magenta and blue ticks are reflection positions of aspirin I and IV, respectively. The calculated fraction of aspirin I is about 33 wt %.

experimental powder pattern (see the [Supporting Information](#) for details).

The structure was refined with TOPAS¹⁷ from synchrotron powder diffraction data (Figure 4). First, the reflection intensities of phase I were extracted by a Pawley fit²⁸ for a data set obtained after full conversion of aspirin IV to I. Then, the crystal structure of phase IV was refined by the Rietveld method ($C_9H_8O_4$, $M_w = 180.16$ g/mol, $\rho_{\text{calc}} = 1.342$ g/cm³, $\lambda =$

0.45336 Å, $2\theta = 1.0$ – 17.5° , $T = 240$ K) with restraints on all bond lengths, valence angles, and planar arylcarboxylate and acetyl groups. To be independent of the vdW-inclusive DFT calculations, the reference values for the Rietveld restraints were taken from the low-temperature single-crystal structure of phase I (CSD code ACSALA14⁵). We refined the orientation of the COOH group from the powder data using a model comprising both in-plane orientations and refining the

occupancies as x and $1 - x$ for each symmetrically independent molecule. The results ($x = 0.97(17)$ for molecule 1 and $0.76(16)$ for molecule 2) indicated the conformation 1a (Figure Sd) for both molecules, which was confirmed by the DFT

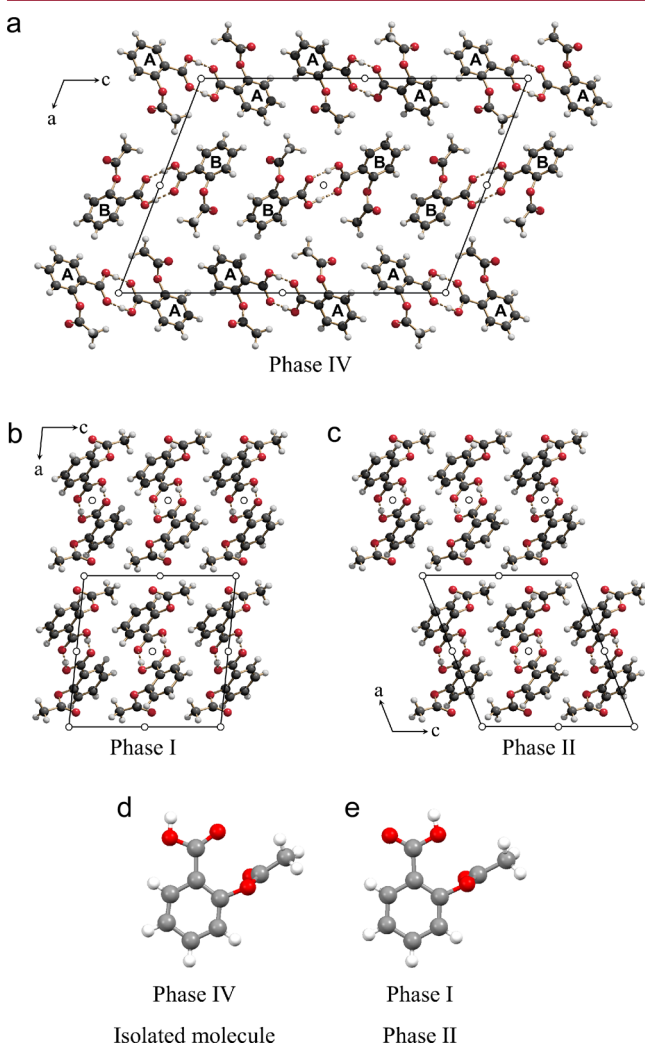


Figure 5. Crystal structures of aspirin: (a) the new phase IV, (b) phase I,³ and (c) phase II.³ View direction for a–c: [010]. Small circles denote the crystallographic inversion centers. In phase IV, the letters A and B denote the two symmetrically independent molecules. (d) Characteristic molecular geometry in the gas phase and in phase IV. (e) Characteristic molecular geometry in phase I and II.

calculations. Hence, only this conformation was used in the final Rietveld refinements. The peak width anisotropy was modeled by second-order spherical harmonics. A correction for preferred orientation was not necessary. The refinement converged with a smooth difference curve (Figure 4), $R_p = 1.75\%$, $R_{wp} = 2.61\%$, $R_{exp} = 1.046\%$ (before background subtraction), $R_p' = 7.015\%$, $R_{wp}' = 7.404\%$, $R_{exp}' = 2.965\%$ (after background subtraction), and a goodness-of-fit of 2.50. The final model of phase IV is $P2_1/c$ with $a = 16.7414(4)$ Å, $b = 4.79496(11)$ Å, $c = 23.8021(8)$ Å, $\beta = 111.082(3)^\circ$, $V = 1782.81(9)$ Å³, $Z = 8$, and $Z' = 2$; CSD accession code: CCDC 1541529 (Figure 5a). As a test, we removed all restraints and performed a free Rietveld refinement. The molecules became distorted, but no atoms (except hydrogens) left their expected domain within the aspirin structure (Figure S6). The final

structure refined with restraints is very close to the structure found in the original search (Figure S7). Periodic models of both structures were expanded to 20-molecule clusters and compared with COMPACT.²⁹ The calculated highest root-mean-square deviation of 0.313 Å confirmed the agreement between experiment and theory.

Compared to aspirins I and II, IV was calculated by optB88-vdw to be ca. 8 kJ/mol higher in energy, while I and II were practically degenerate.³⁰ This value might be overestimated, as we considered only the lattice energy at 0 K. Indeed, a recent study showed that consideration of many body vdW interactions under the harmonic approximation can shift the relative stabilities of I and II by 2.5 kJ/mol at room temperature.³¹ Nevertheless, the observed metastability of IV is consistent with higher free energy.

In the structure of phase IV (Figure 5a), the plane of the acetyl group is nearly perpendicular to the aryl ring plane, as in phases I and II (Figures 5d and e). However, the orientation of the OH group of the carboxyl moiety is on the far side with respect to the acetyl group (Figure 5d), as it is in the gas phase conformation.⁴ In contrast, the OH is on the near side in aspirin I and II (Figure 5e).⁴ If the hydrogen atom was placed on the near side in aspirin IV, the resulting model after optimization by optB88-vdW would be 1.5 kJ/mol higher in lattice energy than the model with H on the far side. The DFT-B88 optimized structure of phase IV is available from CCDC 1541530. As in phases I and II, aspirin IV is comprised of dimers located on the inversion centers of a $P2_1/c$ unit cell. However, in IV, there are two symmetry independent dimers whose planes make angles of 42 and 48° with respect to the [010] direction, whereas the corresponding angles are 60–61° in aspirin I and II. The dimers are arranged in layers in aspirin IV. Aspirin I and II are likewise layered (Figures 5b and c, respectively), but the layer geometry in IV is distinct; phase IV is not another polytype. Phase IV has two symmetrically independent layers, one built by molecule “A” and one by molecule “B” with distinct dimer orientations in the ac plane (Figure 5a). The two layers themselves are quite similar and only slightly influenced by the packing effect of the different arrangements of molecules in the neighboring layers (Figures S8 and S9).

The discovery of a third ambient polymorph of the most well-studied active pharmaceutical ingredient, aspirin, was a consequence of observing the form of spherulitic crystals grown from the melt. Melt crystallization is less common than solution crystallization in pharmaceutical polymorph screening.³² Aspirin IV, of higher potential energy, should lead to faster bioavailability if it can be stored.

■ ASSOCIATED CONTENT

Supporting Information

The Supporting Information is available free of charge on the ACS Publications website at DOI: 10.1021/acs.cgd.7b00673.

Additional experimental details, details of crystal structure prediction, Raman spectrum of Canada balsam, crystallization kinetics, 2D X-ray diffraction powder patterns, lattice energies vs volume for predicted structures, additional drawings of crystal structure, and Hirshfeld surfaces (PDF)

Accession Codes

CCDC 1541529–1541530 contain the supplementary crystallographic data for this paper. These data can be obtained free of

charge via www.ccdc.cam.ac.uk/data_request/cif, by emailing data_request@ccdc.cam.ac.uk, or by contacting The Cambridge Crystallographic Data Centre, 12 Union Road, Cambridge CB2 1EZ, UK; fax: +44 1223 336033.

AUTHOR INFORMATION

Corresponding Authors

*E-mail: qiang.zhu@unlv.edu.

*E-mail: bart.kahr@nyu.edu.

ORCID

Alexander G. Shtukenberg: 0000-0002-5590-4758

Notes

The authors declare no competing financial interest.

ACKNOWLEDGMENTS

This work was supported primarily by the Materials Research Science and Engineering Center (MRSEC) program of the National Science Foundation (NSF) under Award DMR-1420073, and the National Nuclear Security Administration under the Stewardship Science Academic Alliances program through DOE Cooperative Agreement DE-NA0001982. B.K. also thanks the NSF for Awards DMR-1608374, and DMR-1105000. This research used resources of the Advanced Photon Source, a U.S. Department of Energy (DOE) Office of Science User Facility operated for the DOE Office of Science by Argonne National Laboratory under Contract DE-AC02-06CH11357. Computational resources were provided by XSEDE facilities and Center for Functional Nanomaterials at Brookhaven National Laboratory under Contract DE-AC02-98CH10086.

REFERENCES

- (1) Adams, R.; Johnson, J. R. *Laboratory experiments in organic chemistry*; MacMillan: New York, 1927.
- (2) Tawashi, R. *Science* **1968**, *160*, 76.
- (3) Vishweshwar, P.; McMahan, J. A.; Oliveira, M.; Peterson, M. L.; Zaworotko, M. J. *J. Am. Chem. Soc.* **2005**, *127*, 16802–16803.
- (4) Ouvrard, C.; Price, S. L. *Cryst. Growth Des.* **2004**, *4*, 1119–1127.
- (5) Bond, A. D.; Boese, R.; Desiraju, G. R. *Angew. Chem., Int. Ed.* **2007**, *46*, 618–622.
- (6) Bond, A. D.; Boese, R.; Desiraju, G. R. Mixed crystals of form I and form II of acetylsalicylic acid. *Offenlegungsschrift* DE 10 2006 045780 A1, 2008.
- (7) Bond, A. D.; Boese, R.; Desiraju, G. R. *Angew. Chem., Int. Ed.* **2007**, *46*, 615–617.
- (8) Bond, A. D.; Solanko, K. A.; Parsons, S.; Redder, S.; Boese, R. *CrystEngComm* **2011**, *13*, 399–401.
- (9) Crowell, E. L.; Dreger, Z. A.; Gupta, Y. M. *J. Mol. Struct.* **2015**, *1082*, 29–37.
- (10) Bernauer, F. *“Gedrilte” Kristalle*; Gebrüder Bornträger: Berlin, 1929.
- (11) Shtukenberg, A. G.; Punin, Yu. O.; Gujral, A.; Kahr, B. *Angew. Chem., Int. Ed.* **2014**, *53*, 672–699.
- (12) Cui, X.; Shtukenberg, A. G.; Freudenthal, J.; Nichols, S.; Kahr, B. *J. Am. Chem. Soc.* **2014**, *136*, 5481–5490.
- (13) Cui, X.; Rohl, A. L.; Shtukenberg, A.; Kahr, B. *J. Am. Chem. Soc.* **2013**, *135*, 3395–3398.
- (14) Shtukenberg, A. G.; Punin, Yu. O.; Gunn, E.; Kahr, B. *Chem. Rev.* **2012**, *112*, 1805–1838.
- (15) Le Bail, A. *Powder Diffr.* **2004**, *19*, 249–254.
- (16) Boulton, A.; Louër, D. *J. Appl. Crystallogr.* **1991**, *24*, 987–993.
- (17) Bruker AXS. *TOPAS V4: General profile and structure analysis software for powder diffraction data*, User's Manual; Bruker AXS: Karlsruhe, Germany, 2008.

- (18) Zhu, Q.; Oganov, A. R.; Glass, C. W.; Stokes, H. T. *Acta Crystallogr., Sect. B: Struct. Sci.* **2012**, *68*, 215–226.
- (19) Lyakhov, A. O.; Oganov, A. R.; Stokes, H. T.; Zhu, Q. *Comput. Phys. Commun.* **2013**, *184*, 1172–1182.
- (20) Xu, W.; Zhu, Q.; Hu, C. *Angew. Chem., Int. Ed.* **2017**, *56*, 2030–3034.
- (21) Brooks, B. R.; Bruccoleri, R. E.; Olafson, B. D.; States, D. J.; Swaminathan, S.; Karplus, M. *J. Comput. Chem.* **1983**, *4*, 187–217.
- (22) Vanommeslaeghe, K.; Hatcher, E.; Acharya, C.; Kundu, S.; Zhong, S.; Shim, J.; Darian, E.; Guvench, O.; Lopes, P.; Vorobyov, I.; MacKerell, A. D., Jr. *J. Comput. Chem.* **2010**, *31*, 671–690.
- (23) Yu, W.; He, X.; Vanommeslaeghe, K.; MacKerell, A. D., Jr. *J. Comput. Chem.* **2012**, *33*, 2451–2468.
- (24) Aradi, B.; Hourahine, B.; Frauenheim, Th. *J. Phys. Chem. A* **2007**, *111*, 5678–5684.
- (25) Gaus, M.; Goez, A.; Elstner, M. *J. Chem. Theory Comput.* **2013**, *9*, 338–354.
- (26) Kresse, G.; Furthmüller, J. *Phys. Rev. B: Condens. Matter Mater. Phys.* **1996**, *54*, 11169–11186.
- (27) Klimeš, J.; Bowler, D. R.; Michaelides, A. *Phys. Rev. B: Condens. Matter Mater. Phys.* **2011**, *83*, 195131.
- (28) Pawley, G. S. *J. Appl. Crystallogr.* **1981**, *14*, 357–361.
- (29) Chisholm, J. A.; Motherwell, S. *J. Appl. Crystallogr.* **2005**, *38*, 228–231.
- (30) LeBlanc, L. M.; Otero-de-la-Roza, A.; Johnson, E. R. *Cryst. Growth Des.* **2016**, *16*, 6867–6873.
- (31) Reilly, A. M.; Tkatchenko, A. *Phys. Rev. Lett.* **2014**, *113*, 055701.
- (32) Zhu, Q.; Shtukenberg, A. G.; Carter, D. J.; Yu, T.-Q.; Yang, J.; Chen, M.; Raiteri, P.; Oganov, A. R.; Pokroy, B.; Polishchuk, I.; Bygrave, P. J.; Day, G. M.; Rohl, A. L.; Tuckerman, M. E.; Kahr, B. *J. Am. Chem. Soc.* **2016**, *138*, 4881–4889.